Atmospheric Environment Vol. 12, pp. 2151–2158.

0004-6981/78/1101-2151 $02.00/0

AIR POLLUTION IMPLICATIONS OF INVERSION DESCENT IN MOUNTAIN VALLEYS

C. DAVID WHITEMAN and THOMAS B. MCKEE
Department of Atmospheric Science, Colorado State University, Fort Collins, CO 80523, U.S.A.

(*First received* 12 *September* 1977 *and in final form* 15 *March* 1978)

Abstract – Observations of vertical temperature structure in Colorado's deep Gore River Valley indicate that deep inversions that build up within the valley during the night descend into the valley during the hours following sunrise. Direct and indirect evidence indicates that this phenomenon may be a fairly common feature of valley meteorology. This inversion descent will have important implications for dispersal of any pollutant that is emitted into a very stable nocturnal inversion layer since the material may be dispersed after sunrise during inversion descent.

A hypothesis is presented to explain the observations, emphasizing the role of the locally-generated upslope flows in removing mass from under the inversion, resulting in inversion descent. The implications of the hypothesis are investigated using a simple air pollution model based on considerations of mass-continuity and advection. The model predicts pollutant concentration as a function of time for locations along the sidewalls of an idealized valley cross-section.

1. INTRODUCTION

To date, only a few simple air pollution dispersion models have been developed that can routinely be used to predict air pollution concentrations in mountain valley topography. These models, requiring only minimal amounts of input data, but requiring, in many cases, unrealistic assumptions, include the box models and the Gaussian plume model. None of the models is well suited for use with the stable atmospheric structures that often form in mountain valleys. Further, it is the stable atmospheric conditions that are of most interest in many of the applications for which modelling is attempted. Specifically, the break-up of the nocturnal ground-based inversion or stable layer has been identified as a period when high pollutant concentrations reach the ground at the valley bottom and along the sidewalls (Hewson and Gill, 1944). These high concentrations at the ground result from a mechanism, not yet adequately specified, by which the pollutants emitted into and built-up within the stable layer during the night are brought to the ground. An especially critical pollution potential exists where weak synoptic scale flows and clear skies allow an intense stable layer to develop within a valley. In these circumstances the local scale flow within the valley, consisting of up and down-valley and up and down-slope flows, determines the build-up and dispersal of pollutants emitted into the valley.

This paper reports on some recent atmospheric structure observations taken in a mountain valley during inversion break-up, hypothesizes a simple conceptual model to account for the observations, and identifies an air pollution model which can be developed as a consequence of the hypothesis.

2. OBSERVATIONS OF INVERSION BREAK-UP

Whiteman and McKee (1977) presented a series of observations of atmospheric structure taken from the center of the Gore River Valley of Western Colorado using a tethered balloon profiler. The observations were taken during the clear, light-wind weather period of 9 and 10 December 1975 at a location several kilometers above a terrain constriction that effectively kept air from flowing out the end of the valley during the night. Topographical characteristics of the valley and details concerning the balloon profiles are presented in the original article. Table 1 provides a summary of the topographical characteristics of the valley, Fig. 1 presents a cross-section of the valley at the location of the balloon profiler site, and Fig. 2 presents observations taken during the period of inversion break-up.

The first sounding of the morning, initiated at 0831 MST, showed a deep stable layer extending through most of the 475 m depth of the sounding. For comparison, the ridgetops are located at 600 m above the valley floor. By the 0911 MST sounding the steep inversion first seen at 425 m had descended to 340 m. Relatively strong up-valley winds were found above

Table 1. Gore River Valley topographic characteristics

Characteristics	Value
Width of valley floor	0.6 km
Distance between ridge lines	4.5 km
Length of valley	28.0 km
Height of ridge above valley floor	0.6 km
Slope of valley floor	0.02

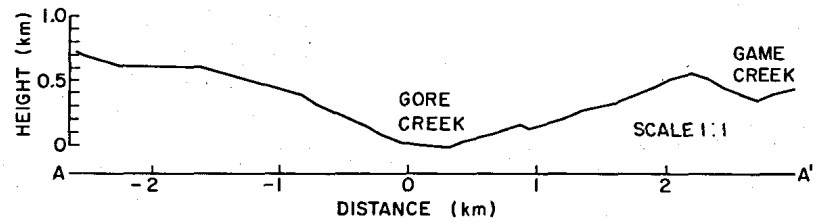

Fig. 1. Cross-section of the Gore River Valley at the site of the tethered balloon profiler.

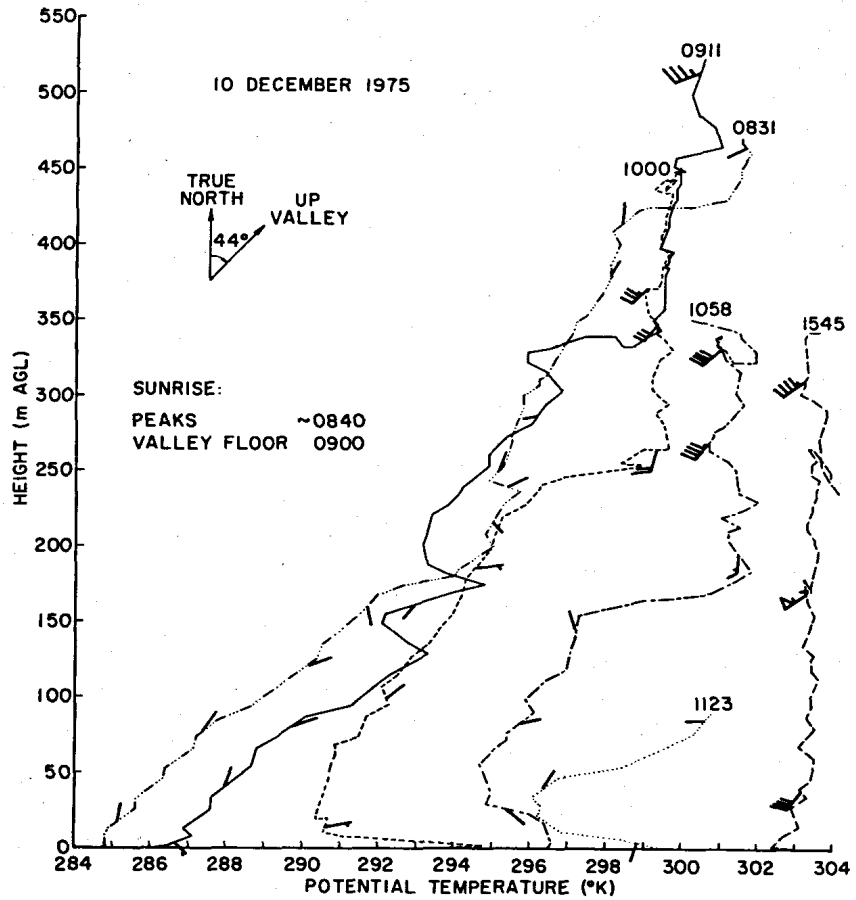

Fig. 2. Tethered balloon profiler observations in the Gore River Valley 10 December 1975. Temperature profiles (up-soundings) are presented for the starting time (MST) indicated. Wind directions and speeds are superimposed on the temperature soundings at points corresponding to heights where wind speed or direction trends change appreciably. A single barb indicates $1\,m\,s^{-1}$. The dotted line indicates a down-sounding which was completed at 1126.

the inversion while light and variable winds prevailed below the inversion. By 1000 MST, insolation was sufficient to form a 20 m deep superadiabatic layer near the ground at the observation site. The top of the inversion layer had continued to descend towards the valley floor, followed closely by continued strong up-valley winds. Weak down-valley winds prevailed in the cold air layer below. Later soundings indicated a slight deepening of the superadiabatic layer, a continued flux of sensible heat into the valley, a descent of the inversion top deeper into the valley, and a replacement of down-valley winds within the valley by up-valley winds from aloft. The inversion dissipated between the down-sounding which ended at 1126 MST (dotted line in Fig. 2 and the 1545 MST up-sounding. Note in Fig. 2 that the inversion top commonly coincides with the point where weak down-valley winds reverse to moderate up-valley winds. The descent of the inversion top, a prominent feature in the observations, is plotted against time in Fig. 3. The inversion descent rate observed during the morning period was nearly constant at about $120\,m\,h^{-1}$. Inversion descent occurred in a similar manner several days later on 16 December 1975 at a site several km further up the valley. On this day the initial nocturnal inversion was not as well developed and the mean descent rate of the inversion

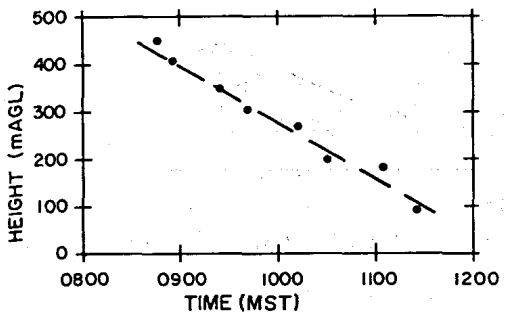

Fig. 3. Height of inversion top vs time.

top was somewhat more rapid – about 160 m h^{-1}. The inversion descent occurred between 0900 and 1130 MST. A parabolic curve provided a significantly better fit to this inversion descent data than a straight line.

In view of the implications that inversion descent may have on temporal changes of turbulent dispersion characteristics within a valley, it seems worthwhile to determine whether there is evidence that this phenomenon occurs in other mountain valleys of the world. A review of the literature has found few published studies of temperature structure evolution in mountain valleys. A recent case study (25 March 1973) of temperature structure in the Mürz Valley of Austria, however, shows the same phenomenon occurring during the same time of day and having a comparable descent rate (Machalek, 1974).

Additional indirect support for the occurrence of the inversion descent phenomenon in other mountain valleys of the world can be obtained from many of the earlier studies of valley wind systems – if we assume that the height of wind reversal corresponds to the height of the inversion top, as roughly indicated in our soundings. Davidson and Rao (1958, 1963), for example, remarked on the downward propagation of up-valley winds into several Vermont valleys during case studies taken during the months June through August. This feature was observed in the hours of the morning after sunrise and descent rates, on the average, were somewhat higher than we observed. Ayer (1961) made a similar observation in the Carbon River Valley of Washington during a summer morning on which cloud cover developed after the observations were begun. Here the rate of descent of the up-valley winds (40–50 m h^{-1}) was lower than we observed. Hewson and Longley (1944) provided additional evidence. They presented wind information taken in the 900 m deep Columbia River Valley of British Columbia for summer months. The averaged information, taken from approximately 1000 pilot balloon observations, indicated that descent of up-valley winds into the valley occurs predominantly during the several hours after 0700 local time at the rate of 70 ± 20 m h^{-1}. Tyson (1967), in his study of the mountain winds over Pietermaritzburg, Natal, in South Africa, has also observed some instances where a nocturnal layer of down-valley winds within a valley dissipates as up-valley winds descend from above during the several hours after sunrise. Other of his observations, however, have shown that the reversal of down-valley winds may be initiated from below or may occur nearly simultaneously through the depth of a valley (see also Defant, 1951).

In summary it appears the descent of up-valley winds into a valley often may be associated with the downward propagation of the top of a temperature inversion. Instances where up-valley winds do not descend from above may be due to the lack of a strongly developed inversion within the valley or the presence or rapid development of a strong wind shear or standing eddy in the upper reaches of the valley. The timing of the inversion breakup and its rate of progress appear to be related to the initiation and progress of insolation within the valley environment.

3. HYPOTHESES FOR INVERSION AND/OR WIND DESCENT

Two hypotheses have previously been offered to account for descent of up-valley winds into a valley during the morning period. Ayer (1961) suggested that up-valley winds descend into a valley as the cold air which built up within the valley during the night slowly drains out the end of the valley. This drainage is possible since the down-slope flows of cold air which fed the cold air mass within the valley during the night are, presumably, interrupted after sunrise by insolation. In order to account for the descent of the top of the cold air mass, this hypothesis requires a net mass divergence from the cold air layer. Due to the topographical constriction in the Gore River Valley below our observation site we observed no drainage or down-valley winds of sufficient speed to turn our anemometer (threshold speed ~ 0.5 m s^{-1}). Thus Ayer's hypothesis cannot be invoked (as he recognized in his paper) to explain inversion descent in this situation. Davidson and Rao (1958) suggested another hypothesis. They postulated that instability develops at ridge top level and that the upper flow then descends into the valley. The more unstable the air at ridge level, the deeper the prevailing flow penetrates into the valley. Presumably this mechanism would erode the top of the cold air layer from above. Our observations, however, show a formidable stable layer at the top of the cold air mass. Gradient Richardson number calculations for this layer show that turbulent mixing of the adjacent layers is strongly suppressed in this region.

In view of the failure of the two previous hypotheses to account for our observations we propose a third hypothesis. Our hypothesis is intended to apply to inversion descent after a clear night in weak synoptic scale flow.

At a time just before sunrise a deep stable layer has built up within the valley. Classical, locally-generated, down-valley winds prevail below the inversion. In the Gore River Valley, the presence of a terrain constriction in the lower reaches of the valley results in

only weak down-valley flows. The top of the stable layer effectively separates the down-valley wind regime below from the winds above the inversion, which are influenced by synoptic-scale pressure gradients but may be modified by topography.

At a time just after sunrise the slopes begin to be heated by insolation, and a thin superadiabatic sublayer forms along the slopes and over the valley bottom. Convection begins in this layer and convective plumes penetrate into the stable cold air mass above. This penetrative convection results in entrainment of mass from the stable layer into the warm sublayer (Ball, 1960; Stull, 1973). An upslope component of motion in the convective sublayer carries the entrained mass up the slopes and out from under the inversion. The principle of mass continuity then requires that the inversion descend. Meanwhile, winds above the inversion become up-valley and increase in strength due to the more rapid warming of the air above the valley relative to air at the same level over the adjacent plains or in a wider portion of the valley down-stream (Cross, 1950). Winds within the stable layer continue to blow weakly down-valley.

Throughout the morning the inversion continues to descend and the stable layer, still containing weak down-valley winds, becomes thinner and thinner. As the stable layer shrinks, up-valley winds progress deeper and deeper into the valley until the inversion layer is completely dissipated. At that time up-valley winds will prevail in the valley volume, and temperature profiles from the center of the valley will indicate nearly constant potential temperature.

The above conceptual model for inversion descent is based on the fundamental concept of mass conservation. If no mass is transported across the inversion top, any mass removed from beneath the inversion by the action of penetrative convection and carried out of the volume by the up-slope circulations will result in a descent of the inversion. The model is specifically developed to account for the Gore River Valley observations although the hypothesized inversion descent mechanism might be expected to operate, perhaps in combination with the previously hypothesized mechanisms, in a well-drained mountain valley. The rate of inversion descent produced by the proposed mechanism will be variable depending on topographic parameters (slope, aspect, etc.) and other factors affecting insolation within the valley (time of year, time of day, surface characteristics, etc.). The size of the valley, especially as it affects the ratio of heated sidewall area to valley volume, will also be important.

In the following sections we develop an air pollution model based on the inversion descent hypothesis and use the model to consider the implications of inversion descent on pollution transport and diffusion.

4. POLLUTION TRANSPORT AND DIFFUSION MODEL

The inversion descent hypothesis of the previous section specifies that, after sunrise, the stable air below an inversion is removed from a valley by downward transport and eventual entrainment into a shallow upslope flow that persists just above the valley floor and heated sidewalls. If the stable air, which developed in the nocturnal flow regime, contains pollutants, the hypothesis can form the framework for a simple valley air pollution transport and diffusion model. Such a model will apply to the post-sunrise hours following the development of a deep, nocturnal, surface-based inversion that develops when synoptic scale flows are weak and secondary flows prevail within a valley.

The model, then, must consider downward transport and subsequent diffusion of pollutants. Pollution in the stable air must be transported downwards in response to inversion descent until it reaches the top of the superadiabatic layer. Once entrained, the pollutants will be diffused rapidly throughout this well-mixed layer. Development of the model will require a specification of inversion descent rate, since this will be the rate at which pollutants within the stable layer are advected towards the ground. A prognostic model for inversion height could be based on a prognosticated insolation field and a parameterization of the rate of mass entrainment from the stable layer into the shallow mixed layer. However, in view of the tentative nature of the inversion descent hypothesis we wish to take the simpler approach of specifying the inversion descent rate on the basis of the observed Vail data. The consequences of the descent of the polluted layer and its subsequent entrainment into the heated sublayer and advection up the sidewalls may then be investigated using the principle of mass continuity.

4.1 *The model*

In accordance with our goal of exploring the basic air pollution implications of the inversion descent hypothesis we wish to construct a simplified model. We begin by considering a valley cross-section (Fig. 4) at a time after sunrise when the mixed layer has attained a constant height H above the valley floor and sidewalls. A row of boxes of height H and of unit depth are placed end to end from the valley center along the valley floor and up the valley sidewall. The length of the individual boxes L is, as yet, unspecified. The pollution concentration χ within the stable layer at the initial time is assumed to be horizontally homogeneous across the stable layer with a vertical profile given by a Gaussian distribution:

$$\chi_{(z)} = \chi_{\max} e^{-\frac{1}{2}\left(\frac{z-D}{\sigma_z}\right)^2}$$

where the maximum concentration $\chi_{\max}$ occurs at height D and the pollutant plume has a standard deviation of σ_z meters.

An inversion descent rate $w = (dh/dt)$ may be specified, and we restrict advection within the stable layer to occur only in the downwards direction in response to inversion descent. Pollutants within the

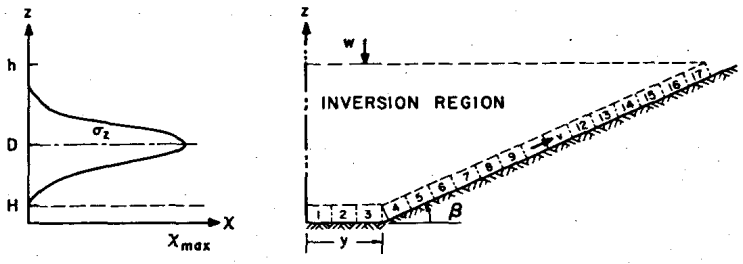

Fig. 4. Schematic diagram of valley model configuration.

stable layer may thus be advected downwards towards the tops of valley floor or sidewall boxes. A knowledge of valley geometry (y = valley half-width and β = slope angle) and inversion descent rate are sufficient to calculate wind speeds v normal to each of the box septa using the equation of mass continuity.

The equation of mass continuity for the pollutant species is then applied for each of the individual boxes in the mixed layer (Fig. 5) at each time step, allowing computation of the net mass of pollutant remaining within the box at the end of the time step. The assumption of uniform mixing of the net mass within each of the boxes after each time step is the mechanism by which diffusion of pollutants through the mixed layer is accomplished in the model. The means of matching the diffusion rate to the actual diffusion rate caused by turbulence in the real slope-flow layer is achieved by choosing the proper combination of time step and box length (Reiquam, 1970).

4.2 *Concentration equations*

Using Fig. 5, the concentration $C_{n,t}$ of pollutant in box n at the end of the tth time step of length Δt is given by a simple pollutant mass balance:

$$C_{n,t} = \frac{M_{\text{initial}} + M_{\text{in}} - M_{\text{out}}}{v_n} \cong \frac{M1_{n,t} + M2_{n,t} + M3_{n,t} + M4_{n,t} - M5_{n,t}}{v_n}$$

where

v_n is the volume of the nth box

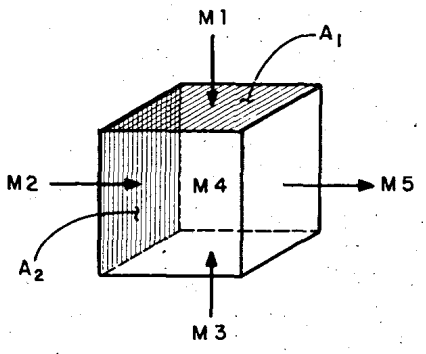

Fig. 5. Schematic diagram of model grid element illustrating mass balance.

$M1_n$ is the mass of pollutant advected into the top of box n during time step Δt.

$M2_n$ is the mass of pollutant advected into box n from the adjacent upstream box $(n-1)$ during time step Δt.

$M3_n$ is the net mass of pollutant introduced into box n during time step Δt from sources and sinks near the ground.

$M4_n$ is the initial mass of pollutant in box n at the beginning of time step Δt.

$M5_n$ is the mass of pollutant advected out of box n into the adjacent downstream box $(n+1)$ at the end of time step Δt after complete mixing of masses $M1$ through $M4$ has taken place within the box.

The separate terms are calculated as follows:

$$M1_{n,t} = \frac{\chi_{\max} v_n}{w\Delta t} \int_{H+(t-1)w\Delta t}^{H+tw\Delta t} e^{-\frac{1}{2}\left(\frac{z-D}{\sigma_z}\right)^2} dz$$

for boxes on the valley floor

$$M1_{n,t} = \frac{\chi_{\max} v_n}{w\Delta t} \int_{H+(j-\frac{1}{2})L\sin\beta+(t-1)w\Delta t}^{H+(j-\frac{1}{2})L\sin\beta+tw\Delta t} e^{-\frac{1}{2}\left(\frac{z-D}{\sigma_z}\right)^2} dz$$

for boxes on the valley sidewall

where

j = special index for boxes on the sidewalls. $j = 1$ corresponds to the lowest box on the sidewall, etc.

$$M2_{n,t} = C_{n-1,t} A_2 v_1 \Delta t$$

where

A_2 = area of box septum

v_1 = wind velocity component into box normal to box septum

$$M3_{n,t} = (Q - S) A_1 \Delta t$$

where

A_1 = area of box top

Q = pollutant emission rate $[ML^{-2}T^{-1}]$

S = pollutant removal rate $[ML^{-2}T^{-1}]$

$$M4_{n,t} = C_{n,t-1} v_n$$

$$M5_{n,t} = \left[\frac{M1_{n,t} + M2_{n,t} + M3_{n,t} + M4_{n,t}}{v_n}\right] A_2 v_2 \Delta t$$

where

v_2 = wind velocity component out of box normal to box septum.

v_1 and v_2 are calculated for each box using an integral form of the continuity equation and assuming that the velocity across the first septum, at the valley center, is zero. Thus, for example, for the first box on the valley floor:

$$\frac{\partial u}{\partial x}+\frac{\partial v}{\partial y}+\frac{\partial w}{\partial z}=0 \quad \text{or} \quad \frac{\partial v}{\partial y}=-\frac{\partial w}{\partial z}$$

$$\int_0^H\int_0^L \frac{\partial v}{\partial y}\,dy\,dz=-\int_0^H\int_0^L \frac{\partial w}{\partial z}\,dy\,dz$$

$$\overline{v_L}-v_0=\frac{L}{H}\overline{w_L}=\frac{Lw}{H}.$$

The absolute velocity normal to a given septum is then determined by summing the velocity changes calculated across each box beginning at the valley center and ending at the septum of interest. Equations for boxes on the slope zone are handled in a similar fashion.

The model is run by integrating forward in time from the initial time and calculating the concentration within each of the boxes. Initial concentrations may be specified for each of the boxes. As the integration proceeds in time the inversion descends deeper and deeper into the valley. This results in some of the boxes on the sidewall being left "high and dry" since no slope flow can be defined for these boxes. This situation is handled by allowing the last calculated concentration within each of the boxes to decay exponentially during successive time steps.

4.3 *Results of model calculations*

Figures 6–9 illustrate the model results for situations corresponding to the 10 December 1975 Vail data. The superadiabatic layer height was taken to be constant at 25 m, and the inversion, initially at 400 m,

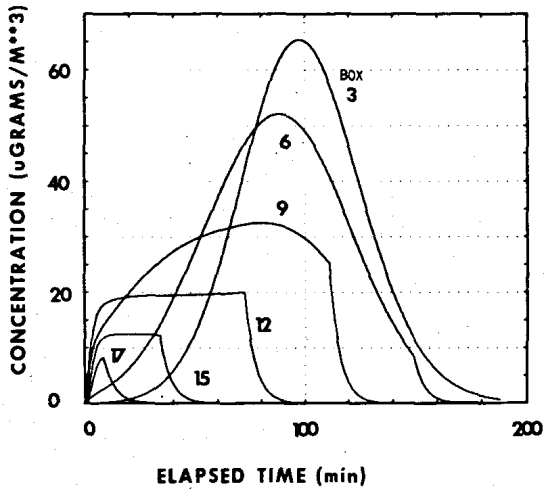

Fig. 6. Concentration ($\mu g\,m^{-3}$) vs elapsed time (min) for selected boxes using $\sigma_z = 50$ m and Vail simulation.

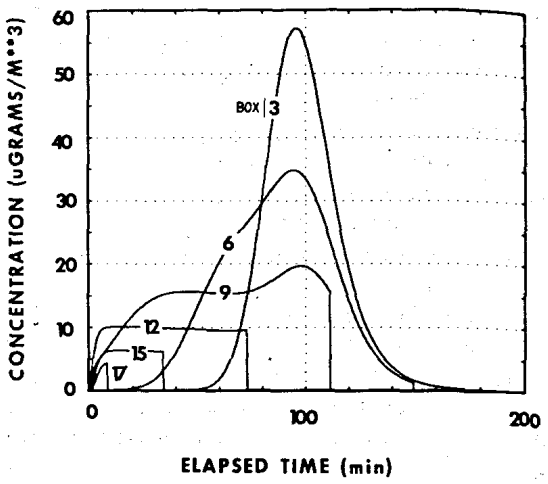

Fig. 7. Same as Fig. 6 except for $\sigma_z = 25$ m.

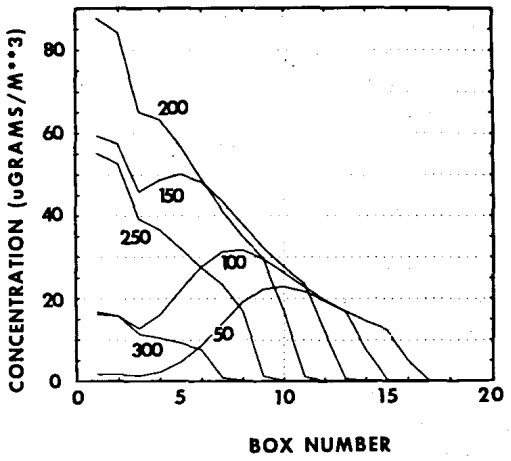

Fig. 8. Concentration vs box number for selected model time steps using $\sigma_z = 50$ m and Vail simulation. 1 time step = 0.5 min.

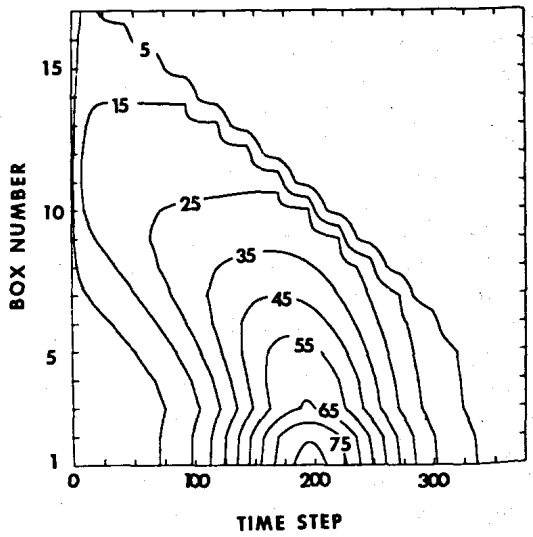

Fig. 9. Contours of concentration ($\mu g\,m^{-3}$) in box number-time step space for Vail simulation with $\sigma_z = 50$ m. 1 time step = 0.5 min.

descended at a constant rate of 120 m h^{-1}. The valley half-width was 300 m and the sidewall sloped upwards at 15 deg. A Gaussian pollution profile was assumed for the stable layer with a maximum concentration of 100 μg m^{-3} at 200 m. The model was run using 375 time steps of 0.5 min duration and a total of 17 boxes of nearly 100 m length. The first 3 boxes were on the valley floor. Initial concentrations within the boxes were taken as zero and no ground sources or sinks were specified.

Figure 6 shows concentration plotted against elapsed time for six of the boxes with $\sigma_z = 50$ m. The curve for box 3, over the valley floor, has a nearly Gaussian shape, as expected from the design of the model – since the major factor at this location will be the downward advection of pollutants rather than advection from the upstream boxes. The peak concentration is less than 100 μg m^{-3}, indicating the combined effects of non-turbulent dispersion processes (divergence of mass) and model pseudo-diffusion. The more rapid rise in the curves for boxes higher up the sidewall is, of course, due to the boxes being closer to the height of maximum concentration of the plume, where entrainment into the boxes and transport from the upstream boxes will result in high concentrations. The occurrence of concentration peaks in boxes 6 and 9 at times near 100 min represents the strong effect of advection of high concentrations up the sidewalls as the plume centerline nears the top of the superadiabatic sublayer over the valley floor. The exponential decay of concentration with time is apparent on all of the curves for the sidewall boxes. The time of initiation of the exponential decay is clearly evident and represents the time when the inversion descends below the elevation of the box.

Figure 7, included for comparison with curve 6, is from a different run in which 2 parameters have been changed – no exponential decay is allowed, and σ_z has been changed to 25 m.

Figure 8 illustrates another type of model output for the $\sigma_z = 50$ m case. Here concentration is given as a function of box number for specific time steps in the integration. For example, at time step number 100, the highest concentration occurs in box number 8. The slight dips in the curves for box number 3 are a consequence of the manner in which the valley "corner" was handled (see Fig. 4).

Figure 9 presents a contour analysis of pollutant concentration as a function of box number and time step for the $\sigma_z = 50$ m case. Figures 6 and 8 are actually 2-dimensional cross-sections of the 3-dimensional surface represented by this figure.

Integral to the air pollution calculations is the calculation of wind velocities across the box septa using the continuity equation for air. Using a constant inversion descent rate for the Vail simulation and assuming density to be constant throughout the valley results in a time-invariant velocity at each of the septa. Velocities vary from zero at the valley center to ~ 2.1 m s^{-1} at the upper septum of the highest (17th) box. This results in an along-box divergence field of 1.3×10^{-3} s^{-1}. Fosberg *et al.* (1976) have recently investigated the effects of such divergence fields on air pollution dispersion by considering modifications to the flux form of the Gaussian plume formulation for use in mountainous terrain. Their estimates of topo-scale divergence values range from $\pm 10^{-4}$ to $\pm 10^{-3}$ s^{-1} with occasional extreme values of 10^{-2} s^{-1}.

Using the Vail data, inversion descent occurs over roughly a 3-h period. Inversion descent would be expected to occur more slowly over a wider valley having the same sidewall and slope-flow characteristics. We may make auxiliary calculations in which the mass removal rate of air from a valley is the same function of inversion height as for the Vail case. These calculations will enable us to determine inversion descent rates for wider (or narrower) valleys and, in the limit, to determine the critical width of a valley for which the inversion will not descend to the ground in a normal length day. The resulting calculations show that a 2 km wide valley will require about 4$\frac{1}{2}$ h to break an inversion, a 4 km wide valley will require nearly 6$\frac{1}{2}$ h and a 6-km wide valley will require over 8 h. Thus an inversion in a valley wider than 6 km may not be broken on a given day and pollutants may remain trapped within the valley for 2 or more days.

Several modifications could be made to the model to make it more realistic. The restriction to horizontal homogeneity of pollutant concentrations within the valley can be changed by specifying different vertical profiles of pollutant concentration above each of the boxes. A horizontal profile specification across the valley could thus be obtained. Additionally, the restriction to a constant depth slope-flow could be easily changed to agree with theoretical predictions of an increase in the depth of this layer with distance up the sidewall (Defant, 1951). A modification could be accomplished to account for cross-valley flow within the stable layer (Gleeson, 1951). Any increase in the sophistication of the model should probably await further observations of the basic phenomenon and testing of the inversion-descent hypothesis.

5. SUMMARY

Observations of temperature structure evolution in the Gore River Valley near Vail, Colorado on mornings following the development of deep surface-based temperature inversions have indicated that the top of the inversion descends towards the ground in the several hours following sunrise. The temporal and spatial variations in turbulence intensity caused by this phenomenon could be expected to influence strongly the dispersion of pollutants within the valley. Despite a scarcity of corresponding temperature structure observations from other valleys of the world there is some evidence, both direct and indirect, that the phenomenon may be a fairly common feature of mountain-

valley meteorology for valleys of certain configurations in synoptic situations leading to inversion formation.

A hypothesis is offered to account for this phenomenon, in which the role of up-slope flows over the valley sidewalls is emphasized in removing mass from the stable air within the inversion. A simple air pollution model is then developed to explore the implications of the hypothesis on air pollution dispersion based on considerations of mass continuity. In this model pollutants are advected downward as the inversion descends until they are entrained into the shallow slope-flow layer. After being entrained into this layer the pollutants are removed from the valley by advection up the slope-flow layer.

The model of pollutant advection and dispersion uses a series of boxes fixed within the slope-flow layer and allows pollutant concentration to be determined as a function of time for any of the boxes. Results are presented in the form of computer-generated graphs for a simulation of the Vail data using an assumed pollution profile. The simulation results in realistic slope-flow velocities ranging up to $2.1\,m\,s^{-1}$ and divergence rates in the slope flow layer of 1.3×10^{-3} s^{-1}. It is emphasized that the air pollution model was developed to consider the implications of a recently-formulated inversion-descent hypothesis. Basic research on the inversion descent phenomenon should be accomplished before the air pollution model is developed further.

Acknowledgements – Dr. M. L. Corrin's encouragement and interest in formulating the air pollution model are gratefully acknowledged. Dr. Gerald J. Mulvey reviewed the manuscript and provided helpful suggestions. Ms. Dorothy Chapman typed the manuscript. The research was partially supported by National Science Foundation Grant ATM76-84405.

REFERENCES

Ayer H. S. (1961) On the dissipation of drainage wind systems in valleys in morning hours. *J. Met.* **18,** 560–563.

Ball F. K. (1960) Control of inversion height by surface heating. *Q. Jl R. met. Soc.* **86,** 483–494.

Cross C. M. (1950) Slope and valley winds in the Columbia River Valley. *Bull. Am. Met. Soc.* **31,** 79–84.

Davidson B. and Rao P. K. (1958) Preliminary report on valley wind studies in Vermont, 1957. Final Report, Contract No. AF19(604)–1971 AFCRC–TR–58–29, College of Engineering, New York University, 54 pp. (Available as PB138594 from NTIS.)

Davidson B. and Rao P. K. (1963) Experimental studies of the valley-plain wind. *Int. J. Air Wat. Pollut.* **7,** 907–923.

Defant F. (1951) Local winds. In *Compendium of Meteorology* (edited by T. M. Malone). American Meteorological Society, Boston, pp. 655–672.

Fosberg M. A., Fox D. G., Howard E. A. and Cohen J. D. (1976) Nonturbulent dispersion processes in complex terrain. *Atmospheric Environment* **10,** 1053–1055.

Gleeson T. A. (1951) On the theory of cross-valley winds arising from differential heating of the slopes. *J. Met.* **8,** 398–405.

Hewson E. W. and Gill G. C. (1944) Meteorological investigations in Columbia River Valley near Trail, B.C., U.S. Dept. of Interior. *Bur. Mines Bull.* **453,** 23–228.

Hewson E. W. and Longley R. W. (1944) *Meteorology, Theoretical and Applied*, pp. 306–310. John Wiley, New York.

Machalek A. (1974) Inversionsuntersuchungen in einem Gebirgstal. *Wetter und Leben* **26,** 157–168.

Reiquam H. (1970) An atmospheric transport and accumulation model for airsheds. *Atmospheric Environment* **4,** 233–247.

Stull R. B. (1973) Inversion rise model based on penetrative convection. *J. atmos. Sci.* **30,** 1092–1099.

Tyson P. D. (1967) Some characteristics of the mountain wind over Pietermaritzburg. *Proc. South African Geog. Soc., Jubilee Conference*, pp. 103–128, Durban.

Whiteman C. D. and McKee T. B. (1977) Observations of vertical atmospheric structure in a deep mountain valley. *Arch. Met. Geoph. Biokl., Ser. A* **26,** 39–50.